



Influence of Paprika Oleoresin Addition on the Structural Properties of Soy Protein Isolate Films

Caroline Furtado Prestes¹ · Livia Alves Barroso¹ · Fernanda Ramalho Procópio¹ · Mariano Michelon² · Miriam Dupas Hubinger¹

Received: 6 October 2022 / Accepted: 7 April 2023 / Published online: 15 May 2023
© The Author(s), under exclusive licence to Springer Science+Business Media, LLC, part of Springer Nature 2023

Abstract

This work evaluated the effect of adding an emulsion containing paprika oleoresin on the properties of soy protein isolate films. Different proportions of the dispersed and continuous phases of the emulsion were studied to define the most stable emulsion to be added to the film. Three films were developed, containing soy protein isolate and glycerol (control film), and added paprika oleoresin emulsion in higher and lower concentrations (0.25% POR and 0.50% POR). The films were evaluated for colorimetric, structural, thermal properties, and molecular interactions. The addition of paprika oleoresin positively impacted the analyzed properties. Films with added oleoresin were more attractive, opaque and have a more resistant barrier to UV/Vis exposure. The emulsion was homogeneously and continuously dispersed, and the films were considered resistant due to the amorphous crystallinity pattern. Characteristic peaks of paprika oleoresin were evidenced by molecular interaction analysis. These results are promising for applications of the films in food products, highlighting the wrapping of meat products such as sausages or bologna.

Keywords Edible films · Emulsion · Color · Oleoresin · Structure

Introduction

Several studies cite the use of macromolecules for producing films, such as proteins, polysaccharides, and lipids; however, the individual insertion of the compounds generates limited filmogenic structures with specific properties (Kumar et al., 2022; McHugh, 1996; Souza et al., 2020; Tirgarian et al., 2023). The development of multicomponent matrices has recently been gaining prominence in edible films. Among their advantages, it was cited an association and improvement in the characteristics of each biopolymer (Paglione et al., 2019; Sanches et al., 2021; Xue et al., 2019). Tirgarian et al. (2023) developed edible oleofilms (composite hydrocolloid–liquid oil films) and observed that the systems could provide better functionality than just hydrocolloid-based films. Xue et al.

(2019) also identified that the hydrophobic nature of essential oils positively impacts the physical, structural, and antioxidant properties of edible films containing emulsion.

Paprika (*Capsicum annuum* L.) oleoresin is a lipophilic matrix from processing pepper fruits. Its phytochemical composition contains glycerides, fat-soluble polyphenols, and carotenoid pigments (Huang et al., 2022; Jimenez-Escobar et al., 2020; Rascón et al., 2011). It is a viscous, brownish-red extract rich in carotenoids, making paprika a common coloring additive in food products (Melgar-Lalanne et al., 2017). However, oleoresins are highly hydrophobic and have low water solubility, which makes not possible their direct application in aqueous film-forming solutions. In addition, taking into account that these compounds are easily oxidized, strategies must be adopted to avoid their degradation and loss of functionality. Therefore, the compounds can be previously delivered in oil-in-water (O/W) emulsions (Procópio et al., 2022b; Reátegui et al., 2017). Emulsions are defined as matrices composed of two immiscible liquids (usually oil and water), which one of them is dispersed as tiny spherical drops (McClements, 2015). O/W emulsions can act as carriers of components that contribute to food stability, flavor, texture, and appearance (Damodaran et al., 2010; Jimenez-Escobar et al., 2020; Liu et al., 2022).

✉ Caroline Furtado Prestes
carolinepresteseng@hotmail.com

¹ Laboratory of Process Engineering, Department of Food Engineering, School of Food Engineering, University of Campinas, Campinas, SP CEP 13083-862, Brazil

² School of Chemistry and Food, Federal University of Rio Grande, Rio Grande, RS CEP 96202-900, Brazil

The incorporation of oily compounds in the form of an emulsion is a trend in research, especially in edible films, as an alternative to improve the effectiveness of the dispersibility of oils in protein media (Ochoa et al., 2017; Ribeiro et al., 2021; Shen et al., 2021). It is necessary to analyze the structural, thermal, and molecular interactions to evaluate the dispersion, effectiveness of homogenization, and incorporation of emulsions in an aqueous medium (Carpiné et al., 2015; Medeiros et al., 2019; Yu et al., 2018).

The use of soy protein isolate (SPI) from defatted soy bran to compose an edible film has a number of advantages. Firstly, this protein is a by-product of the soy chain, which makes its cost more affordable, and represents an added value to this ingredient. Additionally, using paprika oleoresin (POR) presents the differential of being a potential substitute for synthetic additives. In addition to color and flavor, different biological properties arouse the industry's interest in oleoresins, such as promoting antimicrobial, antioxidant, anticancer, and anti-inflammatory activity to products.

Thus, the aim of this work was to add emulsions containing paprika oleoresin to soy protein isolate films and evaluate the effect of the emulsion on the colorimetric, structural, thermal properties, and molecular interactions of the films.

Material and Methods

Material

The materials used for the development of the emulsion were sunflower oil (commercially purchased), POR (Synthite, Valinhos, Brazil), Tween 80 (Sigma-Aldrich, São Paulo, Brazil), and Milli-Q water. SPI (~90% protein, Bremil, Arroio do Meio, Brazil), glycerol, 2 M sodium hydroxide (Dinâmica Química Contemporânea, Indaiatuba, Brazil), and distilled water were included for the preparation of the films. All other chemical reagents were analytical grade.

Development and Characterization of the Emulsion

Paprika Emulsion Preparation

The dispersed phase of the emulsion was composed of sunflower oil and POR, while the continuous phase contained ultrapure water and Tween 80 as the emulsifier. Different fractions of the dispersed and continuous phases were tested, showed in Table 1. The dispersed phase was mixed with the continuous phase using a rotor–stator homogenizer (Model IKA T10 Basic, IKA®-Werke GmbH & Co., KG, Staufen, Germany) at 21,100 rpm for 3 min. Afterward, ultrasound (Model QSonica-Q700, New Town, USA) of 700 W nominal power and a frequency of 20 kHz were applied at 40% amplitude for 5 min. The protocols were modified following the procedure described by Jimenez-Escobar et al. (2020) and Sharma et al. (2021).

Droplet Size, Polydispersity Index, and Zeta Potential

The paprika emulsions were characterized 24 h after homogenization in terms of droplet size average, polydispersity index, and ζ -potential. The analyses were performed by dynamic light scattering using the Litesizer 500 equipment (Anton Paar, Brazil).

Production of Films

Films were prepared using the adapted casting technique (Carpiné et al., 2015). Three formulations were tested: control (C) film without paprika emulsion addition; 0.25% paprika emulsion (0.25% POR) added in the film; and 0.50% paprika (0.50% POR) emulsion added in the film. The film formulation consisted of 6 g of SPI and 1.9 g of glycerol for 100 g of the film-forming solution. According to a preliminary test, SPI was dispersed in distilled water under constant magnetic stirring for 10 min. The pH of the filmogenic solution was adjusted to 10, using NaOH (2 M), and placed under magnetic stirring

Table 1 Formulation and characterization of emulsions containing paprika oleoresin

Sample	Concentration (% w/w)				Droplet size (μm)	Polydispersity index	ζ -potential (mV)
	Sunflower oil	Paprika oleoresin	Tween 80	Water			
E1	9	1	1	89	0.503 ± 0.018^c	0.26 ± 0.03^a	-41.12 ± 1.70^b
E2	7.5	2.5	1	89	0.604 ± 0.025^b	0.27 ± 0.03^a	-31.90 ± 2.94^a
E3	4	1	1	94	0.809 ± 0.013^a	0.26 ± 0.03^a	-35.29 ± 1.52^a
E4	2.5	2.5	1	94	0.581 ± 0.002^b	0.27 ± 0.02^a	-32.20 ± 0.36^a

E1 and E2, emulsions containing 10% of dispersed phase; E3 and E4, emulsions containing 5% of dispersed phase; different letters in the same column indicate a significant difference between the formulations ($p < 0.05$)

for homogenization for 1 h at 70 °C and 450 rpm. Then, glycerol was added and heated at 70 °C for 30 min. The resulting film-forming solution was allowed to stand until it reached room temperature. To prepare the POR film, 0.25% and 0.50% of paprika emulsion were added to the emulsion. Immediately after homogenization, the solution (~ 60 g) was poured into a rectangular plate and dried at 30 °C for 18 h. After drying period, the films were removed, cut into the molds, and placed in desiccators containing saturated NaBr solution (58% RH) for 5 days before analysis. For scanning electron microscopy, atomic force microscopy, and thermal behavior analysis, the samples were placed in desiccators containing silica gel (0% RH and 25 °C) for 7 days.

Characterizations of the Films

Visual Aspect and Thickness

The aspect, homogeneity, and uniformity of the films were observed and described as a visual aspect. The thickness of the films was determined using a digital micrometer (Mitutoyo, Tokyo, Japan) with a scale of 0–25 mm and accuracy of 0.001 mm. The thickness of each film was determined as the average of 10 random measurements.

Color and Opacity

The optical properties of the films were determined by transmittance using an UltraScan VIS colorimeter (HunterLab, Virginia, USA). The scale adopted was CIEL*a*b* and illuminant D-65 (daylight). The measurements were expressed through the parameters L^* (lightness, ranging from black to white), a^* ($+a^*$ = red and $-a^*$ = green), b^* ($+b^*$ = yellow and $-b^*$ = blue), and haze (opacity). The color of the films was expressed as the total color difference (ΔE^*) (Valencia et al., 2016), with L^* , a^* , and b^* being the default color values ($L^* = 97.48$, $a^* = -0.10$, and $b^* = 0.03$) and L , a , and b the values obtained by the experiment.

The total color difference (ΔE) was calculated according to the following equation:

$$\Delta E = \sqrt{(\Delta L^*)^2 + (\Delta a^*)^2 + (\Delta b^*)^2}$$

where ΔL^* , Δa^* , and Δb^* are the differentials between the film color parameter and the color parameter of a standard used as the film background.

The opacity of each sample was determined according to the HunterLab method as a relationship between the opacity of the sample on a black standard and the opacity of the samples in a white standard.

UV/Vis Light Barrier

The barrier property to ultraviolet/visible (UV/Vis) light was determined with a spectrophotometer (UV-M51, UV/Vis Spectrophotometer, Italy), following the methodology described by Reyes et al. (2021). The films were analyzed in strips (10 × 20 mm), fixed in the cuvette, and exposed to the passage of light. Measurements were performed at wavelengths ranging from 200 to 800 nm.

Scanning Electron Microscopy (SEM)

The surface and internal microstructure of the films were performed using a scanning electron microscope (SEM) (LEO Electron Microscopy Leo 440i, Oxford—Cambridge, England), operating with an acceleration power of 10 kV. The samples were immersed in liquid nitrogen to obtain the fracture, fixed on aluminum stubs, and were observed with a magnification of 1000×. Metallic coating (Au) was performed on the samples and then taken to the equipment for analysis.

Atomic Force Microscopy (AFM)

The topography and roughness of the films were performed using an atomic force microscope (Nanosurf EasyScan2 Flex, Switzerland). The samples were submitted to the equipment in the non-contact mode, with a sweep speed of 0.7 s/line, using a tip with a resonance frequency of 190 kHz and a constant force of 48 N/m. The image area was 20 × 20 μm. The mean square roughness (R_{qm}) was calculated using the software Gwyddion (64bit) (Ma et al., 2012).

Crystallinity

The crystallinity of the films was determined by X-ray diffractometer (XRD) (Philips Analytical X-Ray, X'Pert-MPD, Almelo, Netherlands), according to Bergo and Sobral (2007). The film samples (40 mm in diameter) were fixed on aluminum support and placed in the equipment. The measurements were performed at room temperature, with a current of 40 mA and 40 kV. The contact angle ranged from 15° to 30°, with a $K\alpha$ Cu radiation source with $\lambda = 1.54056 \text{ \AA}$.

Fourier Transform Infrared Spectroscopy (FTIR)

The absorption spectra in the infrared region were obtained with a Fourier transform infrared spectrophotometer (FTIR) (Thermo Scientific, Nicolet 6700, Madison, USA), equipped with a Smart OMNI Sampler accessory (by the total attenuated reflectance technique (ATR)). The samples were fragmented in 20 × 10 mm dimensions, fixed in a sample holder, and placed on a crystal for reading. One hundred

twenty-eight scans were performed in the spectral range of 4000–675 cm^{-1} .

Thermal Properties

The thermal properties of the films were determined using a differential scanning calorimeter (DSC1, Mettler Toledo, Schwerzenbach, Switzerland). A small portion of the sample (~5 mg) was collected, weighed in an aluminum dish, and hermetically sealed. The samples were heated from 25 to 300 °C, at a rate of 10 °C/min, under an inert atmosphere of N_2 at a flow rate of 50 mL/min (Sobral & Habitante, 2001; Tessaro et al., 2021).

Statistical Analysis

The means of the results were evaluated by the analysis of variance (ANOVA) and compared through the Tukey's test at the level of 5% significance ($p < 0.05$), using the Statistica 10 software (StatsoftInc., USA).

Results and Discussion

Development and Characterization of the Emulsion

Droplet size, Polydispersity Index, and Zeta Potential

The emulsion was developed to include POR in a dispersed and homogeneous way in the film. The paprika emulsions were characterized in terms of droplet size, ζ -potential, and polydispersity index (Table 1). The emulsion systems containing POR showed droplet sizes ranging between 0.503 and 0.809 μm . It was not possible to verify a significant difference ($p < 0.05$) between the formulations E2 and E4. These results indicated that the droplet diameter is independent of the dispersed phase content, ever since the POR and emulsifier ratio is maintained (2.5:1.0). The results were lower than those cited in the study by Ferraz et al. (2021).

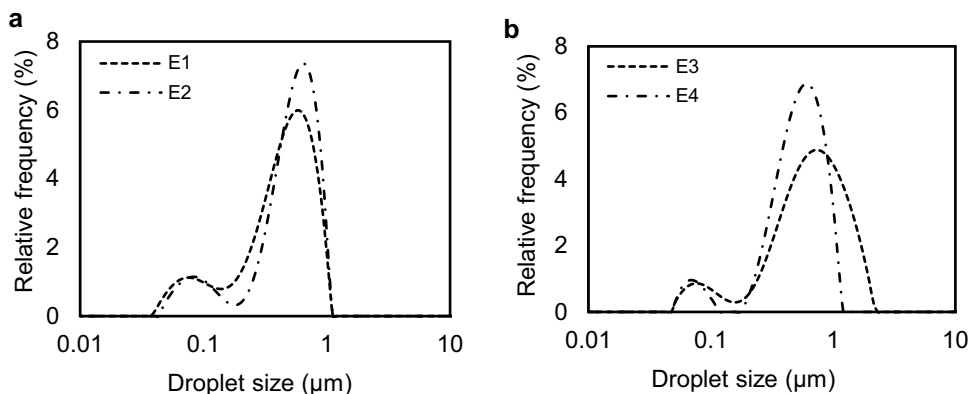
The authors produced emulsions containing paprika and cinnamon oleoresins as dispersed phase, and Arabic gum, whey protein isolate, and maltodextrin in varied concentrations as continuous phase. The average particle diameter was between 0.77 and 41.08 μm .

The ζ -potential, which refers to electrostatic stability, presented negative charges (Table 1). The results ranged from -31.90 to -41.12 mV. The paprika oil resin (POR) is a complex mixture of substances. Due to it, the emulsion with a high content of POR presented less instability and a lower absolute value of zeta potential. However, it was also observed that when the sunflower oil contents started to decrease, the E2, E3, and E4 did not present differences significantly ($p > 0.05$). The high absolute value of the zeta potential indicates smaller particles and a more stable system (Chen et al., 2022). These results can be attributed to the adsorption of negative molecules at the interface, such as OH- species from the aqueous phase and impurities carried through the commercial emulsifier or oils (e.g., free fatty acids) (McClements, 2015; Mun et al., 2007; Sakuno et al., 2008).

The polydispersity index (PDI) was not significantly affected ($p > 0.05$) by the content of oil phase and POR. Shen et al. (2021) studied emulsions for carrying curcumin and obtained polydispersity indices between 0.24 ± 0.02 and 0.37 ± 0.03 . The results obtained by the authors and in this study indicate that the emulsions were uniform and showed homogeneity. According to Yazgan (2022), PDI values lower than 0.5 indicate that the emulsions have a reduced size distribution and are likely to be stable. Regarding the particle size distribution, as seen in Fig. 1, the profiles were bimodal, presenting a larger population with a mode below one μm and a second smaller population with a mode below 0.1 μm . It is possible to affirm that the average size of the particles refers to the largest population, as it presents 90% more occurrences.

The results suggest that the emulsifier allows the development of stable and micrometric scale emulsions, regardless of the amount of oil phase. The tiny droplets obtained in the

Fig. 1 Droplet size distribution of emulsions with the addition of paprika oleoresin, **a** emulsions containing 10% of dispersed phase and **b** emulsions containing 5% of dispersed phase



emulsion, allied to the low polydispersity index, contribute to the increase in the dissolution of the oil phase in a protein medium and the formation of homogeneous films. Therefore, the emulsion selected for application in film-forming solutions was the E4 emulsion.

Characterization of Films

Visual Aspect, Thickness, and Optical Properties

The films were quickly removed from the acrylic plates and presented a smooth and homogeneous surface (Fig. 2). The control film presented a yellowish color, while the films with the addition of POR presented a reddish color. The appearance was continuous, with the emulsion effectively homogenized in the film-forming solution. All films showed malleability (Fig. 2), and light exudation of the oil phase was observed in the film containing the highest percentage of POR.

The average thickness of the films was 0.063 ± 0.019 mm for the control film, 0.086 ± 0.005 mm for the 0.25% POR film, and 0.153 ± 0.019 mm for the 0.50% POR film. The three samples showed a significant difference ($p < 0.05$) with the control film, which showed the lowest thickness value. Due to the absence of emulsion, this fact is associated with the ease of water evaporation during drying. The addition of hydrophobic substances generates an increase in the matrix thickness due to the interactions and reorganization of the molecules during the formation and drying stage of the films (Binsi et al., 2013; Carpiné et al., 2016).

The results referring to the color measurement were expressed through L , a , b , ΔE (color variation), and opacity (haze) (Table 2). The parameters L , a , and b differed statistically ($p < 0.05$) among the three analyzed films. The values indicate that the control film (without POR) showed a more

Table 2 Color parameters and opacity of the analyzed films

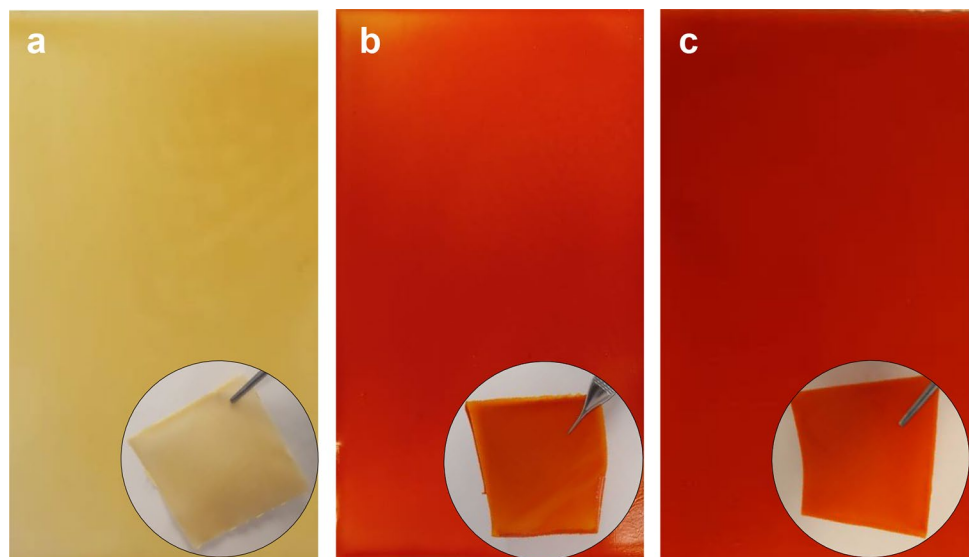
Analysis	C	0.25% POR	0.50% POR
L	55.99 ± 1.07^a	36.14 ± 0.40^b	27.89 ± 0.80^c
a	2.18 ± 0.06^c	32.08 ± 0.77^b	34.85 ± 0.35^a
b	15.71 ± 0.14^c	61.77 ± 0.75^a	47.98 ± 1.38^b
ΔE	44.42 ± 1.03^b	$92.79^a \pm 0.47^a$	91.46 ± 0.24^a
Haze (%)	50.83 ± 0.90^c	55.63 ± 1.11^b	60.53 ± 1.50^a

Mean values (mean value \pm standard derivation). Different letters on the same line indicate a significant difference between the samples ($p < 0.05$)

significant predominance of yellow. The high result of b indicates that the SPI produces intrinsically yellowish films and with little tendency to red color (low value of a). Similar stains were found by Souza et al. (2020), Galus (2018), and Paglione et al. (2019), who produced soy protein-based films. Therefore, the characteristic reddish-orange hue of 0.25% POR and 0.50% POR films comes from carotenoids in POR (Berke & Shieh, 2012). Procópio et al. (2022a) performed the coencapsulation of paprika oleoresin by the spray chilling technique and obtained results identical to those found in our study for the color parameters L , a , and b .

The luminosity of the films (L) varied between 27.89 for the formulation added with the highest amount of oleoresin and 55.99 for the control; that is, the incorporation of the additives darkened the films. According to Belloch et al. (2021), the addition of paprika to dry-cured pork loin affected the color parameters, significantly reducing the “ L ” luminosity and increasing the “ a ” red. The luminosity also can be associated with the water proportion added in the films, which contributes to the lightening of the films; as confirmed in our study, the C sample with higher water

Fig. 2 The visual aspect of control films and films with the addition of paprika oleoresin (POR). **a** Control films without POR; **b** film with 0.25% POR addition; and **c** film with 0.50% POR addition



proportion presented higher luminosity than the other samples (Matheus et al., 2021).

The opacity results indicated that the three formulations differed statistically ($p < 0.05$), with the film with the highest oleoresin addition being the one with the highest opacity. Galus (2018) also observed that the higher the lipid content added (rapeseed oil), the greater the opacity of soy protein-based films. Opaque films can be an attractive protective packaging for foods with photosensitive compounds since they can reduce light transmission (Carpiné et al., 2015).

UV/Vis Light Barrier

The UV/Vis light barrier is desirable in wrapping or packaging materials since ultraviolet (UV) exposure can cause quality problems in photosensitive products (Poverenov et al., 2014). Incorporating POR in the films reduced the transmittance values compared to the control film (Fig. 3). The reduction of transmittance indicates the increase of the UV/Vis barrier of the films, being an excellent alternative for wraps, as it can avoid possible degradations.

The film containing the highest concentration of POR (0.50% POR) showed a transmittance value close to zero (0) in the wavelength range between 200 and 535 nm, indicating a barrier in the analyzed region. This result can be explained by carotenoid pigments, especially capsanthin and capsorubin. Carotenoids absorb in the analyzed wavelength region, so there is a reduction in transmittance (Kim et al., 2016; Minguez-Mosquera et al., 1993).

The structure of POR is rich in unsaturated bonds, and compounds with this structure (double bonds) are responsible for UV/Vis absorption (Berke & Shieh, 2012). Similar results

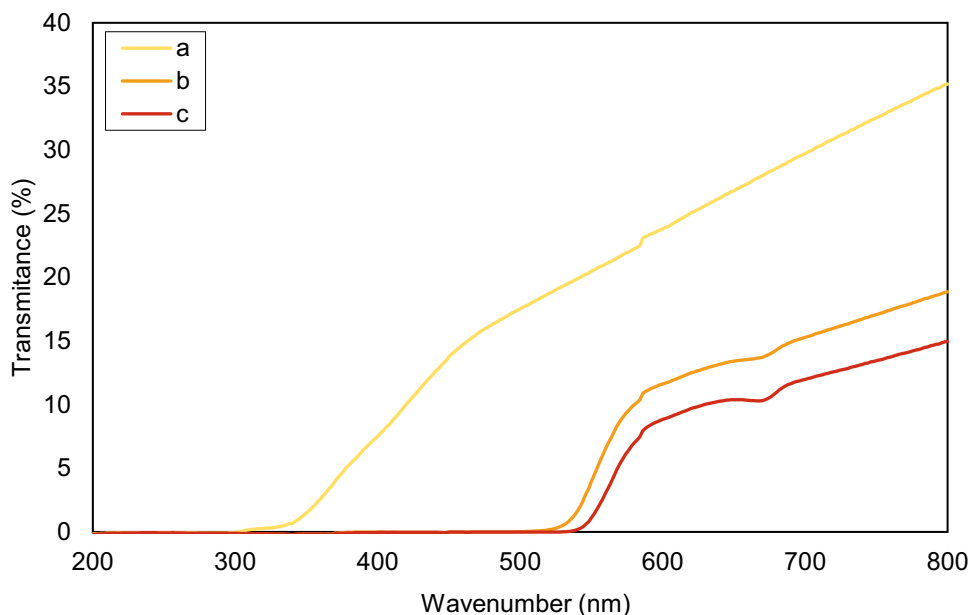
were obtained in gelatin films with turmeric extract, where the film with the highest concentration of turmeric showed a transmittance value between 0.01 and 0.35%, in the wavelength range between 200 and 500 nm, indicating a barrier to radiation in the UV/Vis region (Bitencourt et al., 2014).

Scanning Electron Microscopy (SEM)

The microstructure of the three films can be seen in Fig. 4. The micrographs obtained for the control film (i.e., Fig. 4a) portrayed a smooth, dense, homogeneous surface without pores and cracks, indicating effective homogenization and drying of the film. In Fig. 4b–c, the presence of exposed particles and greater roughness is noticeable compared to the control film. Xue et al. (2019) developed a coating containing essential oil emulsion. The authors observed that the evaporation of water resulted in the carrying of the oil phase to the film's surface, with the droplets becoming apparent in the SEM analysis.

In the figures referring to the cross-section of the films, the image of the control film (Fig. 4d) shows the homogeneous structure inside. In some regions, it is possible to observe certain striations, characteristics of inelastic materials, and brittle when broken. The emulsion films (Fig. 4e–f) showed pores due to air bubbles incorporated during the homogenization and cavitation process. References cited may be applied in future works of vacuum filtration or 2 h of rest before film molding. Patel et al. (2016) and Xue et al. (2019) indicated that the film-forming solution could be filtered under a vacuum. Otoni et al. (2014) suggested letting the film rest for 2 h — before casting the films — to eliminate air bubbles incorporated during emulsion formation.

Fig. 3 UV/VIS spectra of control films and with the addition of paprika oleoresin. **a** Control films without POR; **b** film with 0.25% POR addition; and **c** film with 0.50% POR addition



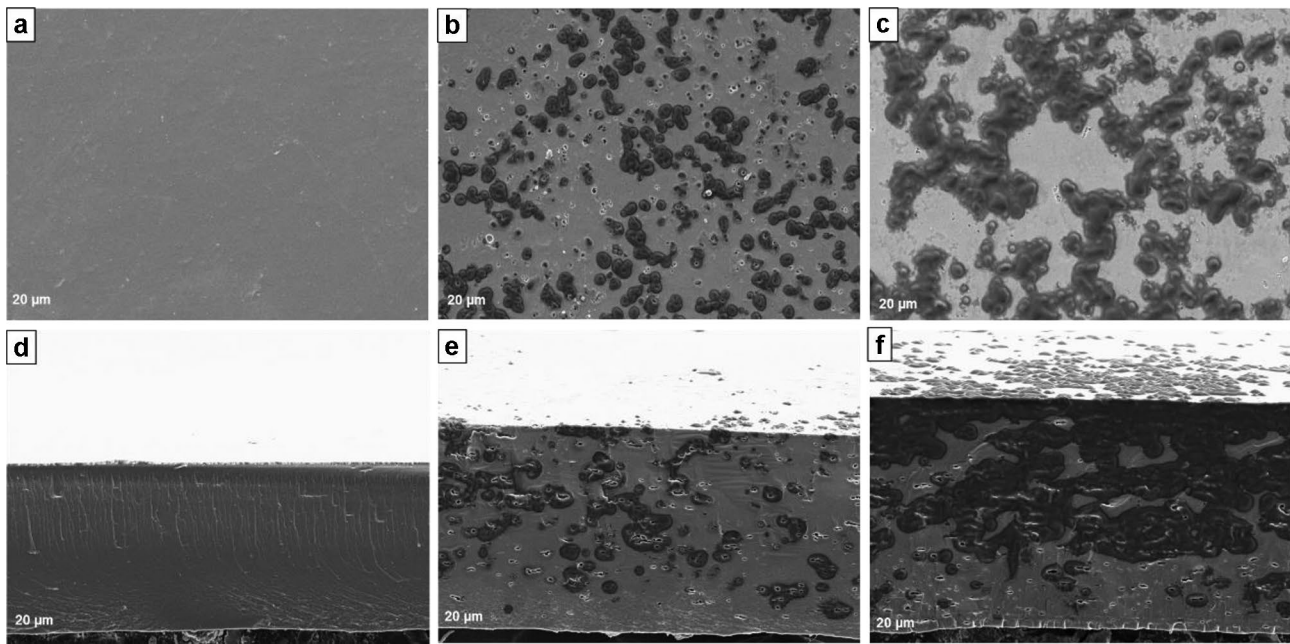


Fig. 4 Scanning electron micrographs (SEM) and cross-section of the surface of the control films and with the addition of POR. SEM of **a** control films without POR; **b** film with 0.25% POR addition; **c** film with

0.50% POR addition. Cross-section of **d** control films without POR; **e** film with 0.25% POR addition; and **f** film with 0.50% POR addition

As well as air bubbles, in Fig. 4e–f, emulsion globules were observed after the drying process. According to Villalobos et al. (2005), the volume fraction of lipids in the dry film and the size of the lipid aggregates are the main factors involved in the degree of heterogeneity in the film matrix. It would be recommended to reduce the droplet diameter at the nanometer level, producing emulsions with a diameter between 20 and 500 nm (Otoni et al., 2014). However, it can be seen in the figures that the emulsion was distributed over the entire surface of the film.

Atomic Force Microscopy (AFM)

Figure 5 presents the flat surfaces and three-dimensional (3D) images of atomic force micrographs. The control film showed the lowest mean square roughness (R_{qm}), 58.45 nm. Films containing 0.25% and 0.50% POR showed 112.6 nm and 203.8 nm, respectively. The film without adding the oil fraction (Fig. 5a) showed a high amount of fine peaks, and the same was reported by Chakravartula et al. (2020). Other authors, when investigating the AFM of SPI, identified that the apparent, more delicate peaks are characteristic of the modification of the structure on a micro- and nanometer scale by the stirring process, together with the surfactant (Acosta-Domínguez et al., 2021; Zhao et al., 2020). It was cited by Souza et al. (2020) that, compared to films without adding extracts, the SPI films added with pinhão extract showed higher roughness, like what was found in our study.

The amount of emulsion added influenced on the film's roughness, and it was found that the more significant the proportion of the oil phase, the greater the surface roughness. This characteristic may be the effect of the slight drag and migration of the emulsion to the surface of the films, and it was observed in SEM images (Fig. 4e–f). Chakravartula et al. (2020) obtained similar results in films containing pitanga leaf extract actives. In the study, the addition of the active compound considerably increased the roughness, indicating insolubility of the particles and the formation of agglomerates during the drying of the film. Other authors have also reported increased roughness by adding hydrophobic materials to biopolymer-based films, such as gelatin film with nanoemulsion of ginger essential oil (Alexandre et al., 2016), zein/chitosan-based film with ginger oil, corn (Shi et al., 2016), and a gelatin-based film contain soybean oil (Dammak et al., 2017).

Crystallinity

The X-ray diffractograms of the three films exhibited a typical amorphous pattern (Fig. 6). In general, adding POR did not cause changes in the structure of the film-forming matrix. All XRD spectra showed similar profiles, with a characteristic amorphous peak in the $2\theta \sim 20^\circ$ region. Ye et al. (2019), for SPI film, recorded amorphous peaks in the regions of 11.4 and 20.1°.

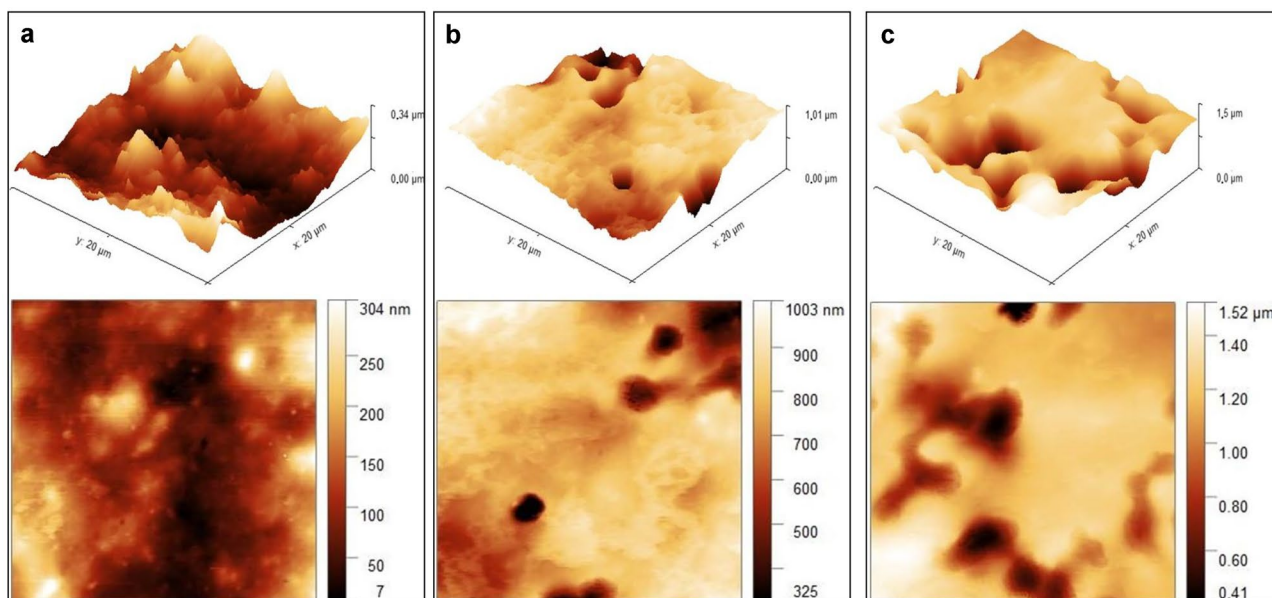


Fig. 5 Surface atomic force and 3D micrographs of control and emulsion-added films. **a** Control films without POR; **b** film with 0.25% POR addition; and **c** film with 0.50% POR addition

The amorphous pattern of the films comes from the proteins, capable of forming three-dimensional structures stabilized by non-covalent interactions and plasticizers. When this network is formed, there is a reduction in interactions between molecules and an increase in the mobility of polymer chains, reducing the crystallinity of the films (Silva et al., 2020).

The amorphous structure of the films may also be related to the presence of glycerol. The addition of a plasticizer reduces the ordered structure characteristic of crystalline materials by increasing the distance between macromolecules. Higher molecular mobility then occurs, which minimizes the crystallization of the film components. Therefore,

the amorphous state of the films is desired since crystalline matrices have weak and fragile structural characteristics (Vieira et al., 2011).

Fourier Transform Infrared Spectroscopy (FTIR)

The functional groups were analyzed through the infrared spectra to evaluate the effect of the emulsion on the interactions of the film components at the molecular level (Fig. 7). The spectra varied between 4000 and 675 cm^{-1} . The absorption peak between 3295 and 3270 cm^{-1} showed typical elongation of the OH and NH groups indicated by amide A (responsible for hydrogen bonds). There are also

Fig. 6 X-ray diffraction in control films and with paprika oleoresin addition. **a** Control films without POR; **b** film with 0.25% POR addition; and **c** film with 0.50% POR addition

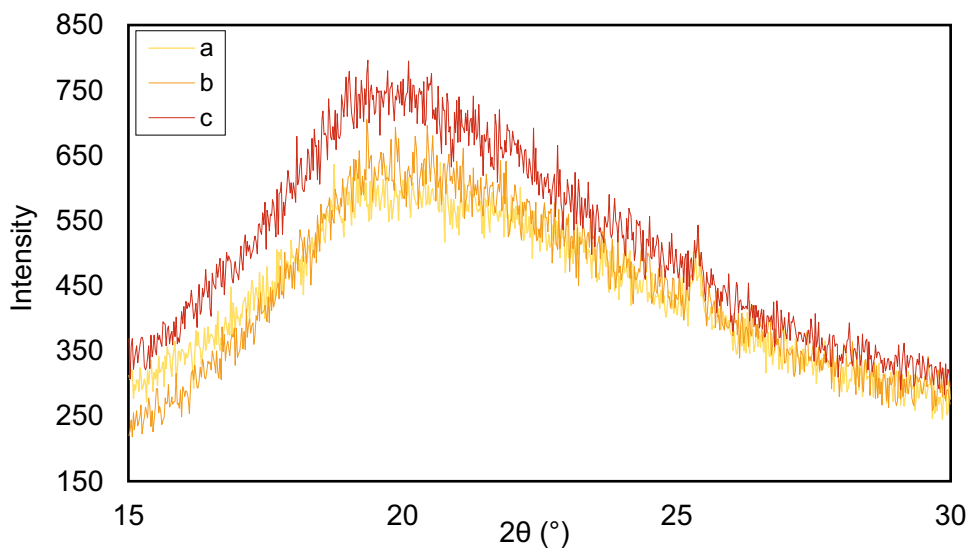
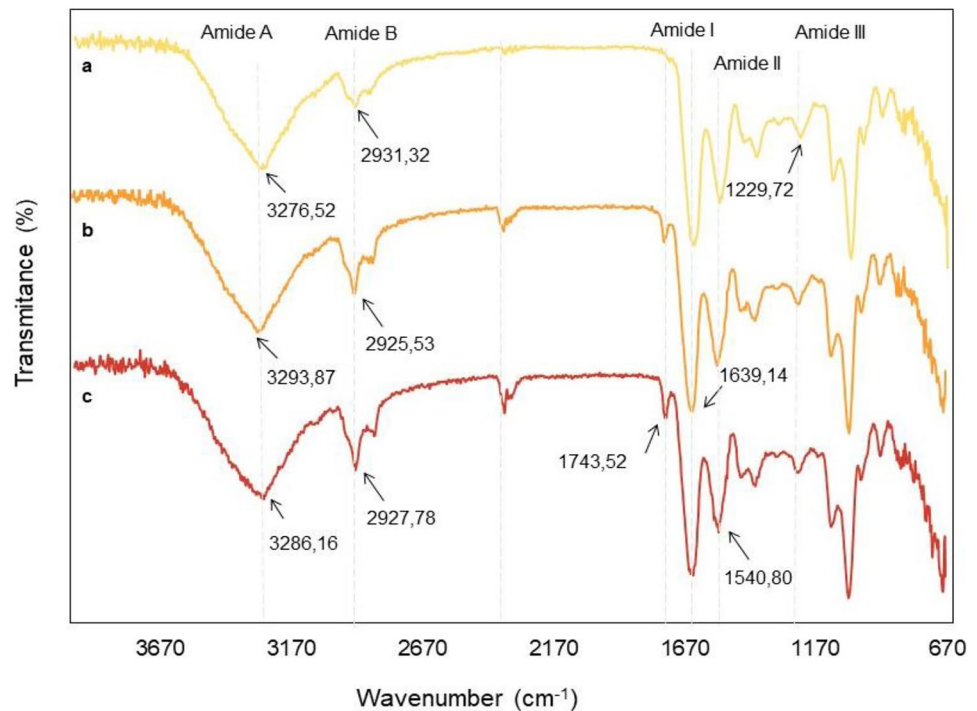


Fig. 7 Fourier transform infrared spectroscopy in control films and with the addition of paprika oleoresin. **a** Control films without POR; **b** film with 0.25% POR addition; and **c** film with 0.50% POR addition



visible peaks in the three samples varying between 2932 and 2925 cm^{-1} , indicating the presence of the methyl group CH and NH_3 (amide B). The same peaks characteristic of hydroxyl OH groups and CH groups were found by Saberi et al. (2017) in films of natural plant extracts. Jincheng and Sihao (2010) report the presence of a peak in the 2900 cm^{-1} region, characteristic of the CH group present in capsaicin.

The appearance of stretching in films with the addition of POR (i.e., Fig. 7b–c) was evidenced at 1743 cm^{-1} , typical of C=O stretching. This peak is characteristic of ketones, aldehydes, and phenolics in the fatty acids of oils and was also reported by Galvin-King et al. (2020). In the present study, the C=O (amide I), N–H (amide II), and C–N (amide III) elongation curvatures were observed at 1639 cm^{-1} , 1540 cm^{-1} , and 1229 cm^{-1} , respectively. The peak equivalent to amide III is also highlighted by the CH_2 group, characteristic of the presence of glycerol in the medium.

Figure 7 shows that the peaks referring to amide B and amide I in the 0.25% POR and 0.50% POR films showed more good stretching properties than the control, which may indicate interaction of the compounds present in the oleoresins with the matrix of the film. Ekhlasi et al. (2016) identified the amide B and amide I peaks when evaluating the spectra of capsaicin from chili pepper (*Capsicum annuum* L.).

Thermal Properties

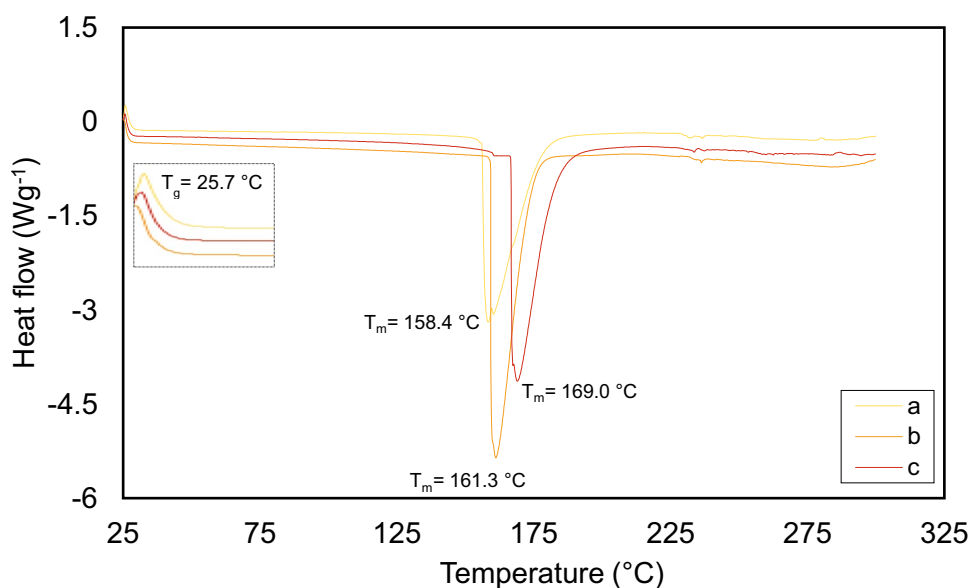
Thermal transitions in films are analyzed to verify the film's performance, such as the fragility and strength of the

material. When subjected to temperature variation, polymers can trigger structural changes resulting from the rupture of chemical bonds or complete degradation of the chains (Carpiné et al., 2015; Lucas et al., 2001). The thermal properties, or glass transition temperature (T_g) and melting point temperature (T_m), were measured by DSC and are shown in Fig. 8. The three films showed a glass transition (T_g) followed by endothermic peaks (T_m), associated with the fusion of macromolecules.

The glass transition occurred approximately at the same temperature for the three films studied, equivalent to 25.7 °C. Research evaluating SPI films with the addition of glycerol observed that in samples containing 1.9% (in 100 g of the film) of glycerol, glass transition results appeared at temperatures of 18.28 and 48.96 °C. The researchers attributed the glass transitions to the 7S and 11S fractions of the soy protein, respectively (Mo & Sun, 2002). Hu et al. (2021), when evaluating SPI films emulsified with essential oil, found that T_g had no significant variation between control films and films with the addition of essential oil, suggesting that T_g was not affected by emulsification.

On the other hand, the addition of hydrophobic compound had a subtle influence on the melting temperatures (T_m) of the films. Ma et al. (2012) observed that films emulsified with olive oil showed an endothermic peak shift, similar to the result of this work. SPI was the compound evidenced mainly by the DSC, so that thermal transitions may be associated with protein denaturation. In the case of SPI, the denaturation temperature (T_d) is generally referred to as the denaturation

Fig. 8 DSC thermal curves of control and paprika oleoresin added films. **a** Control films without POR; **b** film with 0.25% POR addition; and **c** film with 0.50% POR addition



temperature of the two main component fractions of soy protein, glycine (7S) and β -conglycinin (11S). When in solution, the T_d of these fractions is located between 80–95 °C and 60–80 °C, respectively, for 11S and 7S. The T_d of a protein is generally not dependent on its concentration when in solution, where this temperature is usually below 100 °C. However, at low water contents, T_d increases, and endothermic peaks are shifted to temperatures above 100 °C (Kitabatake et al., 1989).

In the present study, as the film contained low water content, referring to 9.0%, it can be inferred that near 100 °C, there was a loss of the residual water contained in the raw material, and the events recorded in the endothermic peaks (T_m); Fig. 8 represents the temperature of protein denaturation.

Zhang et al. (2021) found an endothermic peak between 150 and 180 °C and attributed it to the destruction of hydrogen bonds between molecules in the SPI film. Tang et al. (2009) considered the same — the irreversible endothermic peak with high temperature is due to the breaking of the hydrogen bonds between the proteins and the plasticizer. The authors considered that molecular disruption was the main reason for retaining protein structure in SPI films.

Conclusion

Paprika oleoresin can be incorporated into edible soy protein isolate films to improve their optical, structural, and light barrier properties. Despite the challenge of including hydrophobic oleoresins in an aqueous medium, the emulsion technique favored the dispersion of the oil phase in the protein medium. The color of the films with the addition of paprika oleoresin was more attractive than the control. The film with 0.50% POR showed better opacity and barrier to UV/Vis light. This

feature is essential when the film is intended to be a wrapper for a food product, since the increased barrier to light inhibits oxidative reactions. The infrared spectrum identified the peaks of capsanthin and capsorubin compounds, characteristic of paprika oleoresin. In short, the paprika oleoresin films showed potential for use in food products, highlighting the application for meat products, such as mortadella and sausages. Future studies are needed and suggested, especially the application and industrial scale-up, to improve the operational conditions and evaluate the compatibility between the film and the final product.

Author Contribution Caroline Furtado Prestes: conceptualization; formal analysis; methodology; validation; visualization; writing, original draft; and writing, review and editing. Lívia Alves Barroso: formal analysis, validation, and writing, review and editing. Fernanda Ramalho Procópio: formal analysis, methodology, validation, and writing, review and editing. Mariano Michelon: supervision and writing, review and editing. Miriam Dupas Hubinger: supervision; writing, review and editing; project administration; and funding acquisition.

Funding This work was funded by “Conselho Nacional de Desenvolvimento Científico e Tecnológico (CNPq)” with the Master and PhD assistantships (Caroline Furtado Prestes #131515/2020–9, Fernanda Ramalho Procópio #141111/2018–6, Call CNPq/MCTI/FNDCT N° 18/2021—Process #408117/2021–4) and the productivity grant (Miriam Dupas Hubinger #306461/2017–0). Partial financial support was received from FAPESP through the thematic project FAPESP 2019/27354–3. The work also received support from “Coordenação de Aperfeiçoamento de Pessoal de Nível Superior” for the project and PhD assistantships (CAPES-Brazil; Finance code 001, Lívia Alves Barroso #88887.479715/2020–00) and the Fundação de Amparo à Pesquisa do Estado do Rio Grande do Sul (Process #21/2551–0000600–5) for funding this research project.

Data Availability The authors confirm that the data supporting the findings of this study are available within the article.

Declarations

Conflict of Interest The authors declare no competing interests.

References

- Acosta-Domínguez, L., Cocotle-Ronzón, Y., Alamilla-Beltrán, L., & Hernandez-Martinez, E. (2021). Effect of a cryogenic treatment in the microstructure, functional and flow properties of soy protein isolate. *Food Hydrocolloids*, 119, 106871. <https://doi.org/10.1016/j.foodhyd.2021.106871>
- Alexandre, E. M. C., Lourenço, R. V., Bittante, A. M. Q. B., Moraes, I. C. F., & Sobral, P. J. A. (2016). Gelatin-based films reinforced with montmorillonite and activated with nanoemulsion of ginger essential oil for food packaging applications. *Food Packaging and Shelf Life*, 10, 87–96. <https://doi.org/10.1016/j.foodhyd.2016.10.004>
- Belloch, C., Neef, A., Salafia, C., López-Diez, J. J., & Flores, M. (2021). Microbiota and volatile of dry-cured pork loins manufactured with paprika and reduced concentration of nitrite and nitrate. *Food Research International*, 149, 110691. <https://doi.org/10.1016/j.foodres.2021.110691>
- Bergo, P., & Sobral, P. J. A. (2007). Effects of plasticizer on physical properties of pigskin gelatin films. *Food Hydrocolloids*, 21(8), 1285–1289. <https://doi.org/10.1016/j.foodhyd.2006.09.014>
- Berke, T. G., & Shieh, S. C. (2012). Capsicum cultivars. In *Handbook of Herbs and Spices* (pp. 116–130). Elsevier. <https://doi.org/10.1533/9780857095671.116>
- Binsi, P. K., Ravishankar, C. N., & Srinivasa Gopal, T. K. (2013). Development and characterization of an edible composite film based on chitosan and virgin coconut oil with improved moisture sorption properties. *Journal of Food Science*, 78(4), E526–E534. <https://doi.org/10.1111/1750-3841.12084>
- Bitencourt, C. M., Fávoro-Trindade, C. S., Sobral, P. J. A., & Carvalho, R. A. (2014). Gelatin-based films additivated with curcuma ethanol extract: Antioxidant activity and physical properties of films. *Food Hydrocolloids*, 40, 145–152. <https://doi.org/10.1016/j.foodhyd.2014.02.014>
- Carpiné, D., Dagostin, J. L. A., Bertan, L. C., & Mafra, M. R. (2015). Development and characterization of soy protein isolate emulsion-based edible films with added coconut oil for olive oil packaging: Barrier, mechanical, and thermal properties. *Food and Bioprocess Technology*, 8(8), 1811–1823. <https://doi.org/10.1007/s11947-015-1538-4>
- Carpiné, D., Dagostin, J. L. A., de Andrade, E. F., Bertan, L. C., & Mafra, M. R. (2016). Effect of the natural surfactant *Yucca schidigera* extract on the properties of biodegradable emulsified films produced from soy protein isolate and coconut oil. *Industrial Crops and Products*, 83, 364–371. <https://doi.org/10.1016/j.indcrop.2016.01.014>
- Chakravartula, S. S. N., Lourenço, R. V., Balestra, F., Bittante, A. M. Q. B., Sobral, P. J. do A., & Rosa, M. D. (2020). Influence of pitanga (*Eugenia uniflora* L.) leaf extract and/or natamycin on properties of cassava starch/chitosan active films. *Food Packaging and Shelf Life*, 24, 100498. <https://doi.org/10.1016/j.foodhyd.2020.100498>
- Chen, M., Wang, L., Xie, B., Ma, A., Hu, K., Zheng, C., et al. (2022). Effects of high-pressure treatments (ultra-high hydrostatic pressure and high-pressure homogenization) on bighead carp (*Aristichthys nobilis*) myofibrillar protein native state and its hydrolysis. *Food and Bioprocess Technology*, 15(10), 2252–2266. <https://doi.org/10.1007/s11947-022-02878-1>
- Dammak, I., de Carvalho, R. A., Trindade, C. S. F., Lourenço, R. V., & do Amaral Sobral, P. J. (2017). Properties of active gelatin films incorporated with rutin-loaded nanoemulsions. *International Journal of Biological Macromolecules*, 98, 39–49. <https://doi.org/10.1016/j.ijbiomac.2017.01.094>
- Damodaran, S., Parkin, K. L., & Fennema, O. R. (2010). *Química de Alimentos de Fennema* - 4ª ed. - Editora Artmed.
- Ekhlas, E. A. K., Zahra, A. N. H., & Jenan, A.-A.A. (2016). FT-IR identification of capsaicin from callus and seedling of chilli pepper plants *Capsicum annuum* L. in vitro. *International Journal of Multidisciplinary and Current Research*, 4, 1144–1146.
- Ferraz, M. C., Procópio, F. R., de Figueiredo Furtado, G., Munhoz Moya, A. M. T., Cazarin, C. B. B., & Hubinger, M. D. (2021). Cinnamon and paprika oleoresin emulsions: A study of physicochemical stability and antioxidant synergism. *Food Research International*, 150, 110777. <https://doi.org/10.1016/j.foodres.2021.110777>
- Galus, S. (2018). Functional properties of soy protein isolate edible films as affected by rapeseed oil concentration. *Food Hydrocolloids*, 85, 233–241. <https://doi.org/10.1016/j.foodhyd.2018.07.026>
- Galvin-King, P., Haughey, S. A., & Elliott, C. T. (2020). The detection of substitution adulteration of paprika with spent paprika by the application of molecular spectroscopy tools. *Foods*, 9(7), 944. <https://doi.org/10.3390/foods9070944>
- Huang, P., Yu, Q., Feng, X., Ma, C., & Kan, J. (2022). Optimization of accelerated solvent extraction of paprika oleoresin and its effect on capsaicinoid and carotenoid composition. *Journal of Food Composition and Analysis*, 110, 104589. <https://doi.org/10.1016/j.jfca.2022.104589>
- Hu, Y., Shi, L., Ren, Z., Hao, G., Chen, J., & Weng, W. (2021). Characterization of emulsion films prepared from soy protein isolate at different preheating temperatures. *Journal of Food Engineering*, 309, 110697. <https://doi.org/10.1016/j.jfoodeng.2021.110697>
- Jimenez-Escobar, M. P., Pascual-Mathey, L. I., Beristain, C. I., Flores-Andrade, E., Jiménez, M., & Pascual-Pineda, L. A. (2020). In vitro and in vivo antioxidant properties of paprika carotenoids nanoemulsions. *LWT*, 118, 108694. <https://doi.org/10.1016/j.lwt.2019.108694>
- Jincheng, W., & Sihao, C. (2010). Preparation and characterization of microcapsules containing capsaicin. *Journal of Applied Polymer Science*, 116(4), 2234–2241. <https://doi.org/10.1002/app.31684>
- Kim, J.-S., An, C. G., Park, J.-S., Lim, Y. P., & Kim, S. (2016). Carotenoid profiling from 27 types of paprika (*Capsicum annuum* L.) with different colors, shapes, and cultivation methods. *Food Chemistry*, 201, 64–71. <https://doi.org/10.1016/j.foodchem.2016.01.041>
- Kitabatake, N., Tahara, M., & Doi, E. (1989). Denaturation temperature of soy protein under low moisture conditions. *Agricultural and Biological Chemistry*, 53(4), 1201–1202. <https://doi.org/10.1271/bbb1961.53.1201>
- Kumar, A. V., Hasan, M., Mangaraj, S., Pravitha, M., Verma, D. K., & Srivastav, P. P. (2022). Trends in edible packaging films and its prospective future in food: A review. *Applied Food Research*, 2(1), 100118. <https://doi.org/10.1016/j.afres.2022.100118>
- Liu, F., Liang, X., Yan, J., Zhao, S., Li, S., Liu, X., et al. (2022). Tailoring the properties of double-crosslinked emulsion gels using structural design principles: Physical characteristics, stability, and delivery of lycopene. *Biomaterials*, 280, 121265. <https://doi.org/10.1016/j.biomaterials.2021.121265>
- Lucas, E. F., Soares, B. G., & Monteiro, E. C. (2001). Caracterização de polímeros determinação de peso molecular e análise térmica - 1ª ed. - E-Papers.
- Matheus, J. R. V., de Assis, R. M., Correia, T. R., da Costa Marques, M. R., Leite, M. C. A. M., Pelissari, F. M., et al. (2021). Biodegradable and edible film based on persimmon (*Diospyros kaki* L.) used as a lid for minimally processed vegetables packaging. *Food and Bioprocess Technology*, 14(4), 765–779. <https://doi.org/10.1007/s11947-021-02595-1>

- Bioprocess Technology*, 13(6), 998–1008. <https://doi.org/10.1007/s11947-020-02454-5>
- Tang, C.-H., Xiao, M.-L., Chen, Z., Yang, X.-Q., & Yin, S.-W. (2009). Properties of cast films of vicilin-rich protein isolates from Phaseolus legumes: Influence of heat curing. *LWT - Food Science and Technology*, 42(10), 1659–1666. <https://doi.org/10.1016/j.lwt.2009.05.020>
- Tessaro, L., Lourenço, R. V., Martelli-Tosi, M., & do Amaral Sobral, P. J. (2021). Gelatin/chitosan based films loaded with nanocellulose from soybean straw and activated with “Pitanga” (*Eugenia uniflora* L.) leaf hydroethanolic extract in W/O/W emulsion. *International Journal of Biological Macromolecules*, 186, 328–340. <https://doi.org/10.1016/j.ijbiomac.2021.07.039>
- Tirgarian, B., Farmani, J., & Milani, J. M. (2023). Edible oleofilms with high vegetable oil content obtained from novel soy protein isolate/gelatin/chitosan nanofiber emulgels. *Food Hydrocolloids*, 134, 108082. <https://doi.org/10.1016/j.foodhyd.2022.108082>
- Valencia, G. A., Lourenço, R. V., Bittante, A. M. Q. B., & do Amaral Sobral, P. J. (2016). Physical and morphological properties of nanocomposite films based on gelatin and Laponite. *Applied Clay Science*, 124–125, 260–266. <https://doi.org/10.1016/j.clay.2016.02.023>
- Vieira, M. G. A., da Silva, M. A., dos Santos, L. O., & Beppu, M. M. (2011). Natural-based plasticizers and biopolymer films: A review. *European Polymer Journal*, 47(3), 254–263. <https://doi.org/10.1016/j.eurpolymj.2010.12.011>
- Villalobos, R., Chanona, J., Hernández, P., Gutiérrez, G., & Chiralt, A. (2005). Gloss and transparency of hydroxypropyl methylcellulose films containing surfactants as affected by their microstructure. *Food Hydrocolloids*, 19(1), 53–61. <https://doi.org/10.1016/j.foodhyd.2004.04.014>
- Xue, F., Gu, Y., Wang, Y., Li, C., & Adhikari, B. (2019). Encapsulation of essential oil in emulsion based edible films prepared by soy protein isolate-gum acacia conjugates. *Food Hydrocolloids*, 96, 178–189. <https://doi.org/10.1016/j.foodhyd.2019.05.014>
- Yazgan, H. (2022). Antimicrobial activities of emulsion-based edible solutions incorporating lemon essential oil and sodium caseinate against some food-borne bacteria. *Journal of Food Science and Technology*, 59(12), 4695–4705. <https://doi.org/10.1007/s13197-022-05551-9>
- Ye, Q., Han, Y., Zhang, J., Zhang, W., Xia, C., & Li, J. (2019). Bio-based films with improved water resistance derived from soy protein isolate and stearic acid via bioconjugation. *Journal of Cleaner Production*, 214, 125–131. <https://doi.org/10.1016/j.jclepro.2018.12.277>
- Yu, Z., Sun, L., Wang, W., Zeng, W., Mustapha, A., & Lin, M. (2018). Soy protein-based films incorporated with cellulose nanocrystals and pine needle extract for active packaging. *Industrial Crops and Products*, 112, 412–419. <https://doi.org/10.1016/j.indcrop.2017.12.031>
- Zhang, H., Wang, L., Li, H., Chi, Y., Zhang, H., Xia, N., et al. (2021). Changes in properties of soy protein isolate edible films stored at different temperatures: Studies on water and glycerol migration. *Foods*, 10(8), 1797. <https://doi.org/10.3390/foods10081797>
- Zhao, H.-S., Ma, Z., & Jing, P. (2020). Interaction of soy protein isolate fibrils with betalain from red beetroots: Morphology, spectroscopic characteristics and thermal stability. *Food Research International*, 135, 109289. <https://doi.org/10.1016/j.foodres.2020.109289>

Publisher's Note Springer Nature remains neutral with regard to jurisdictional claims in published maps and institutional affiliations.

Springer Nature or its licensor (e.g. a society or other partner) holds exclusive rights to this article under a publishing agreement with the author(s) or other rightsholder(s); author self-archiving of the accepted manuscript version of this article is solely governed by the terms of such publishing agreement and applicable law.